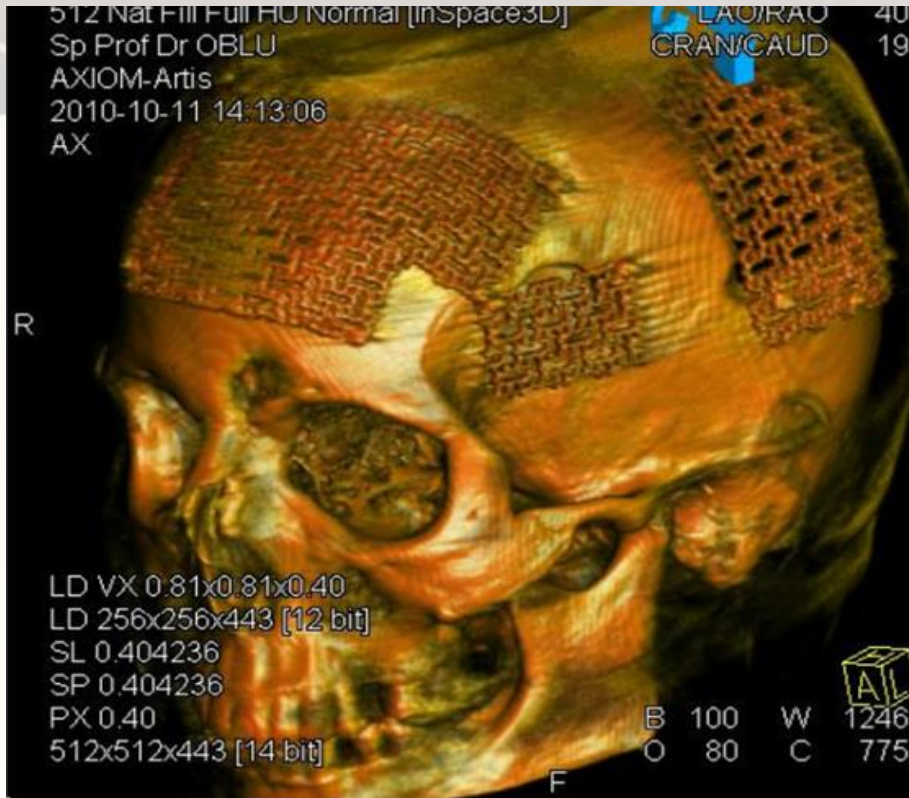


Prototype cranial mesh prostheses produced by Laser Additive Manufacturing

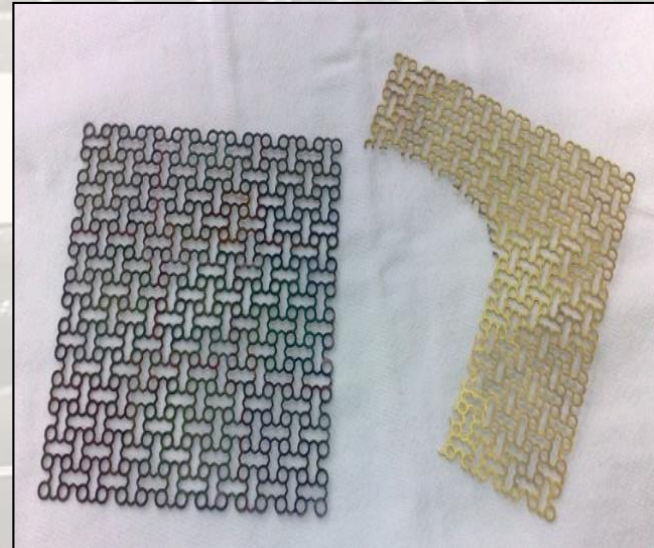
D. Chioibasus^{1,2}, A.C. Popescu¹

¹ Center for Advanced Laser Technologies - CETAL,
National Institute for Lasers, Plasma and Radiation Physics, Magurele, Romania
² University POLITEHNICA of Bucharest, Doctoral School of the Faculty of Applied Science,
Splaiul Independentei 313, Bucharest, Romania

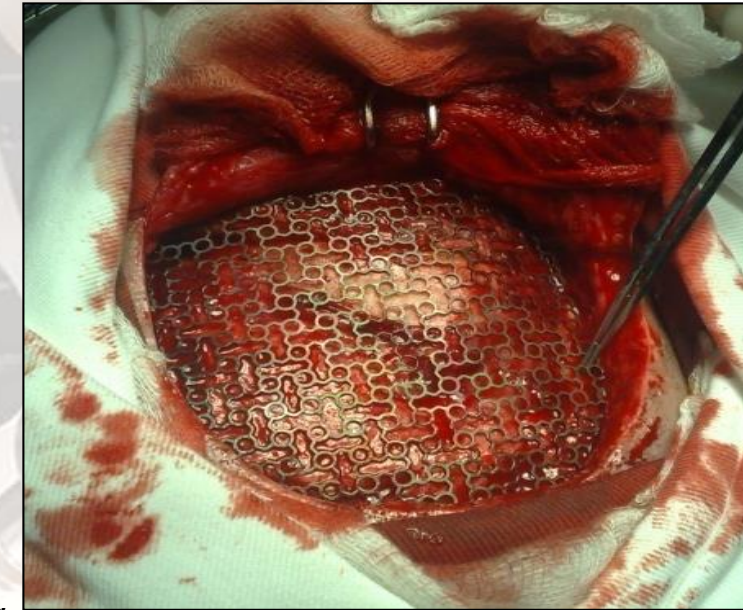




Tomografie computerizata a unui pacient cu proteze craniene de Ti



Proteza de Ti craniana neacoperita (dreapta) si acoperita (stanga) cu un film subtire de sticla bioactiva



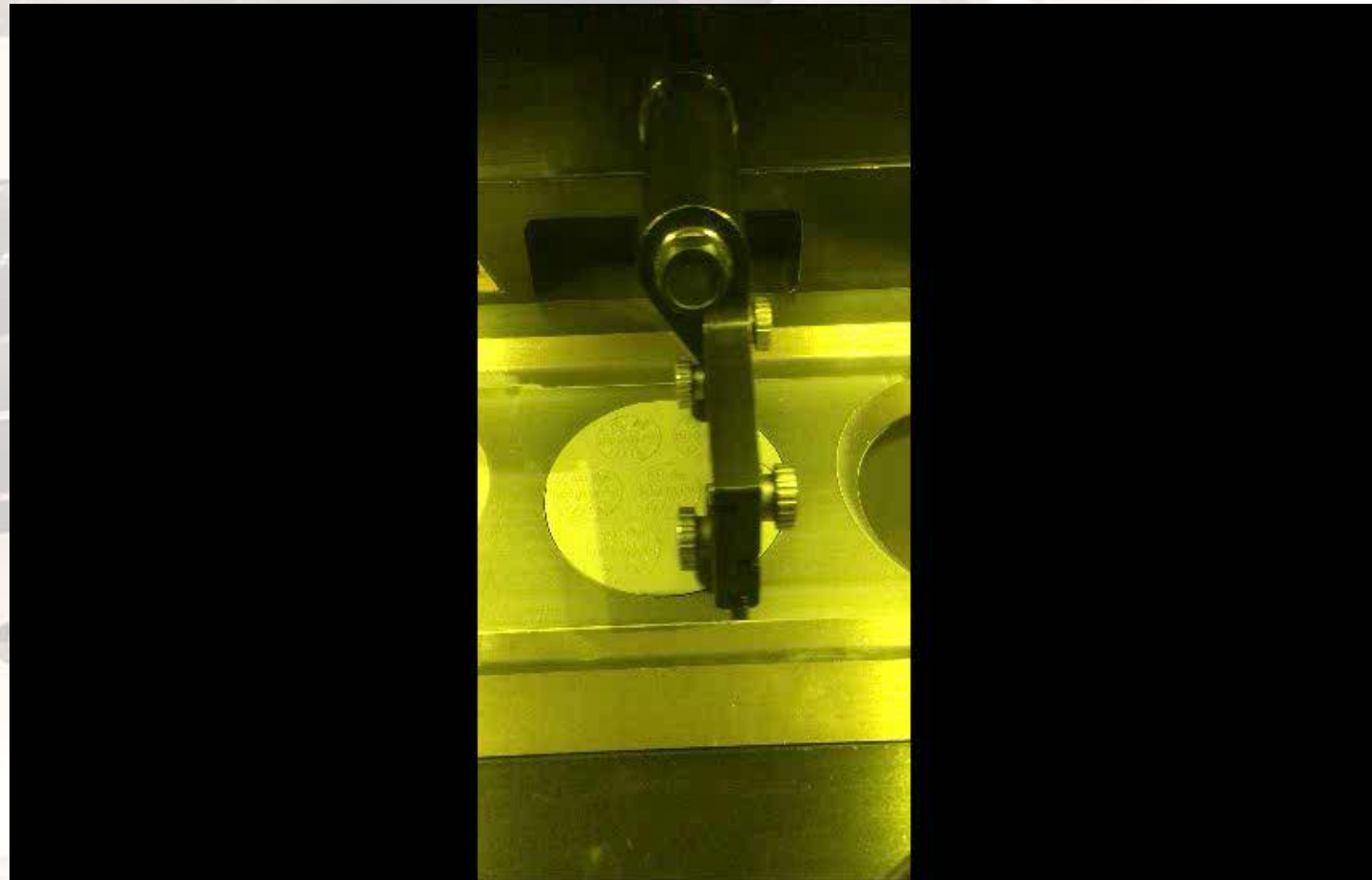
Interventie chirurgicala pentru reparatie craniana utilizand o proteza de Ti



Selective Laser Melting



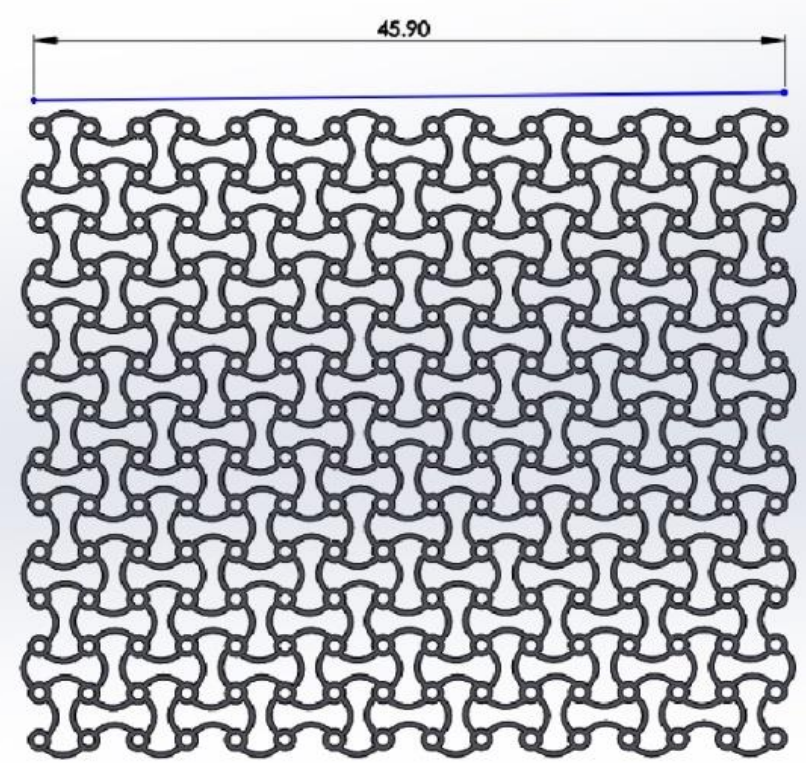
M270 machine for 3D printing of metallic materials by SLM method



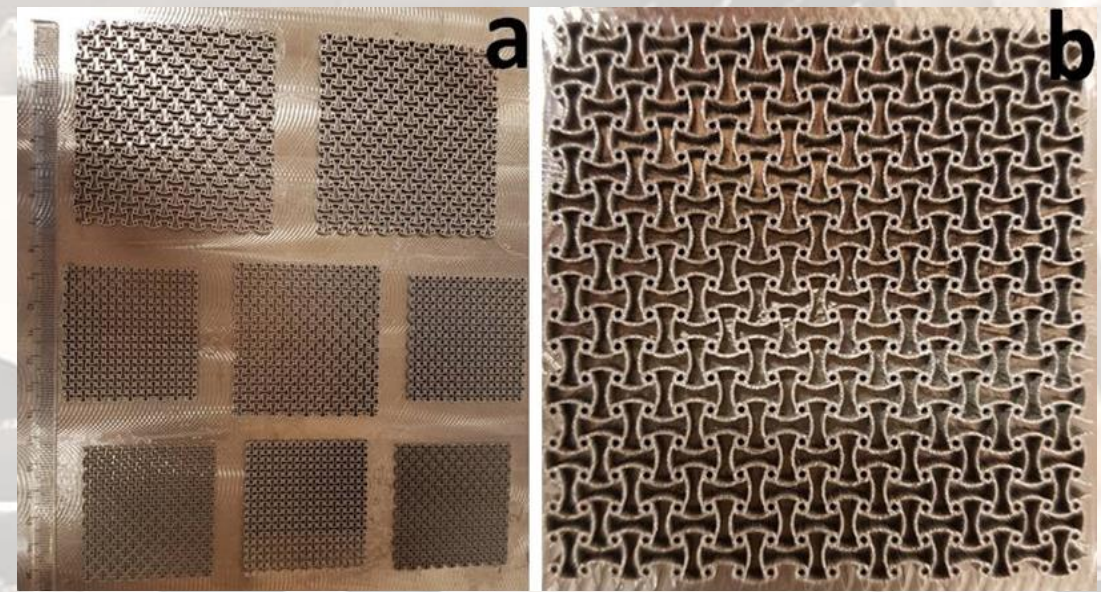
$L_p = 90 \text{ W}$ $S_s = 450 \text{ mm/s}$ $L_s = 100 \mu\text{m}$



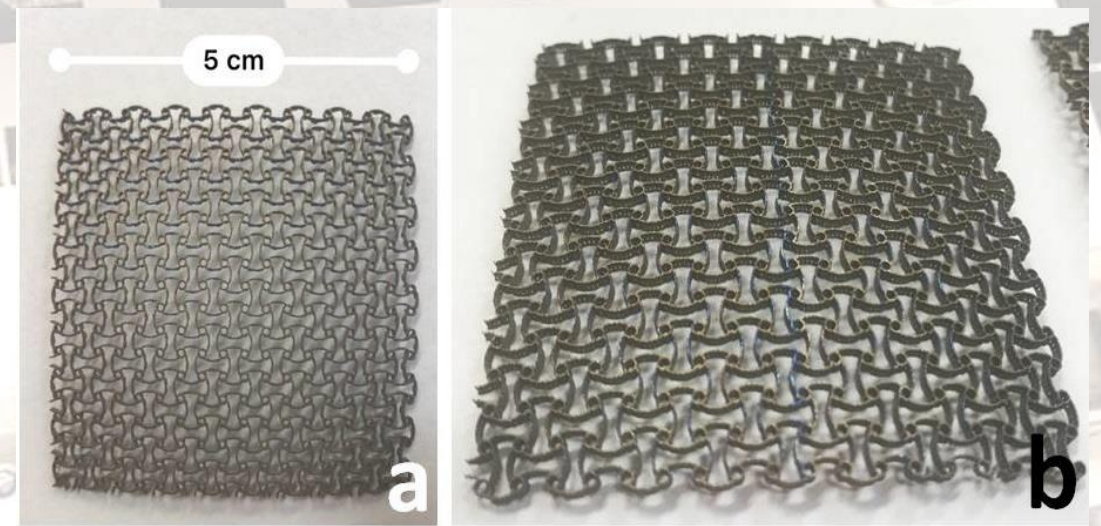
Cranial meshes fabricated by SLM



2D image of a cranial prosthesis model made in Solid Works for 3D printing by SLM



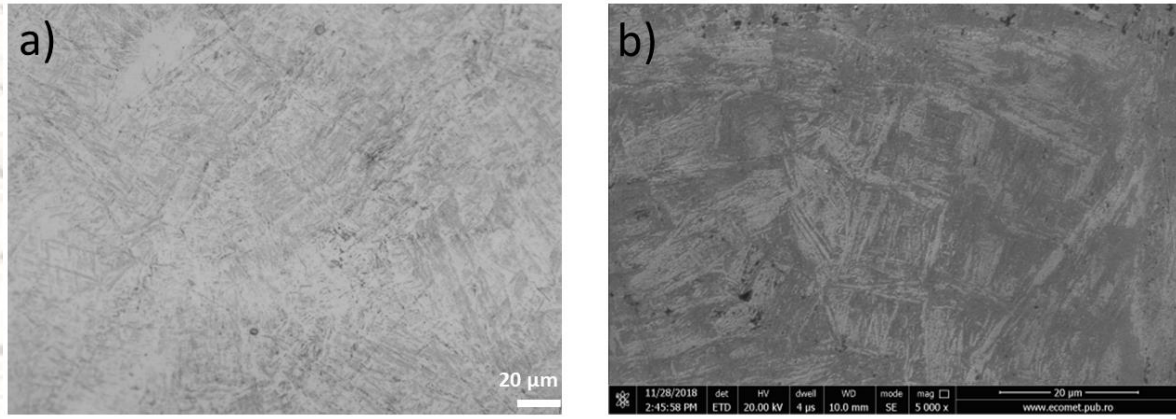
a) 3D image with 3D printed prostheses at different scales of the initial technical drawing and b) detail with the cranial mesh made by SLM



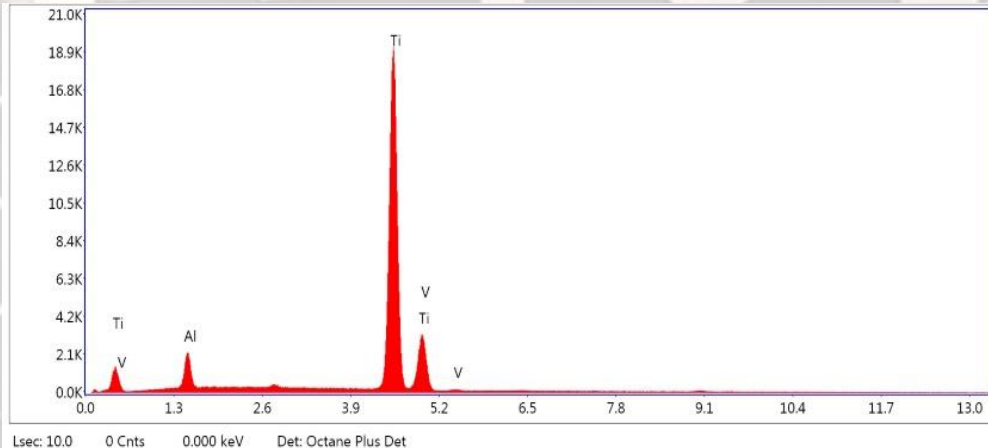
a) Cranial mesh 3D printed by SLM after cutting off growth support and b) detail of the final prosthesis



Metallographic characterization of 3D printed material by SLM

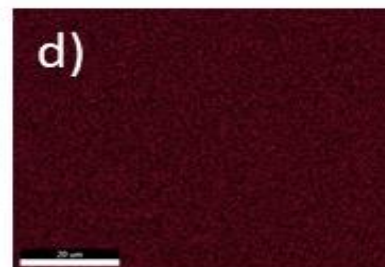
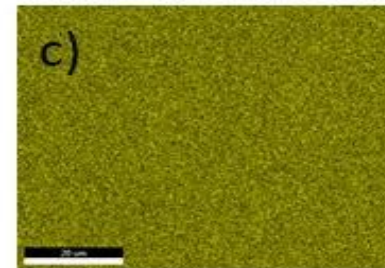
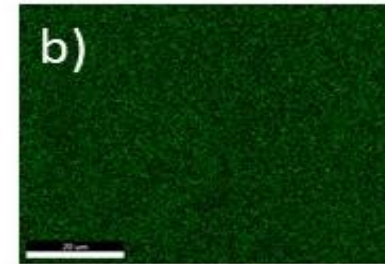
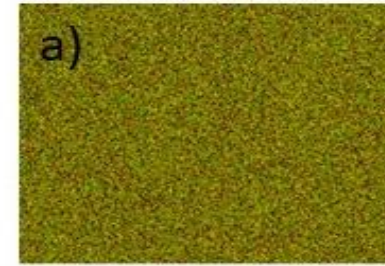


a) optical microscopy M = 100x; b) SEM M = 500x of the Ti6Al4V sample 3D printed using the SLM method



Ti=90.18% wt
Al=5.61% wt
V=4.21% wt

EDXS characteristic spectrum of a Ti6Al4V sample 3D printed using the SLM method



Composite maps produced by the characteristic radiation a) Ti-Kα, Al-Kα, V-Kα global, b) Al-Kα, c) Ti-Kα, d) V-Kα

Microhardness: 391±5 HV

Coating the prosthesis with a bioactive ceramic layer

- Hydroxyapatite of animal origin prepared at the Marmara University, Istanbul, Turkey
- Bovine and sheep bones
- Thin layers coating → Radio-Frequency Magnetron Sputtering → large and uniform coverage area

Method parameters:

$P \sim 3 \times 10^{-3}$ Pa

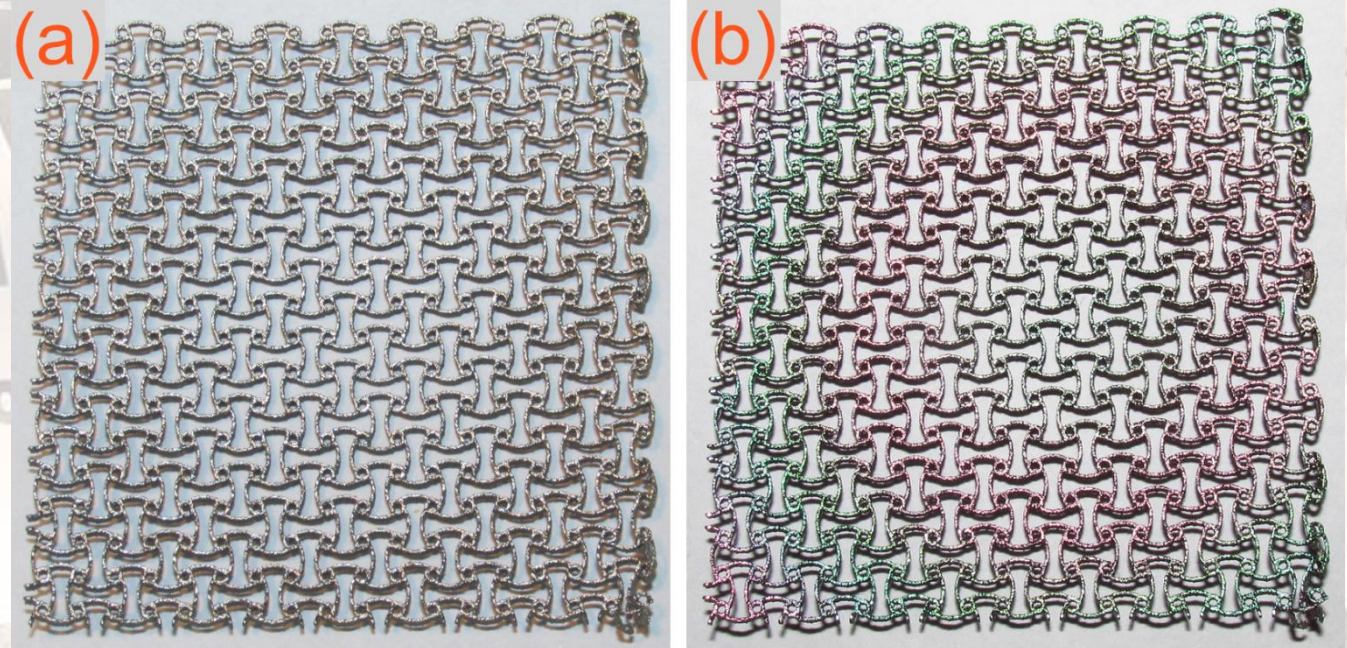
$P_{Ar} = 0.3$ Pa

$T = 150^\circ\text{C}$

$D = 35$ mm

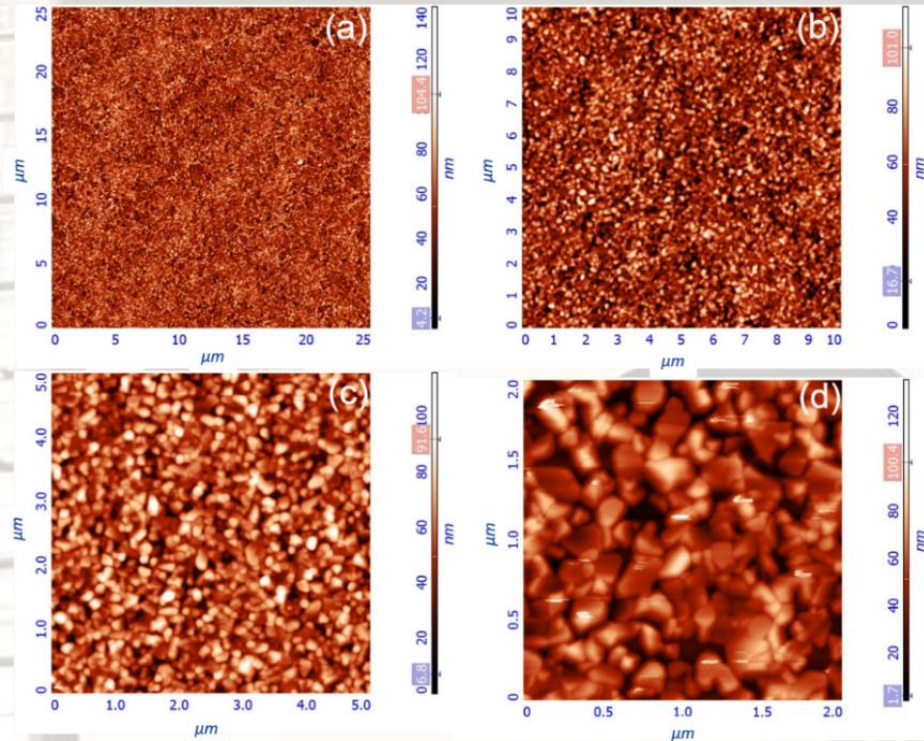
Layer thickness = 600 nm (~ 4 nm/min)

To induce the crystallization of deposited HAB films
 → thermal treatments at $500^\circ\text{C}/1\text{h}$ in air were applied



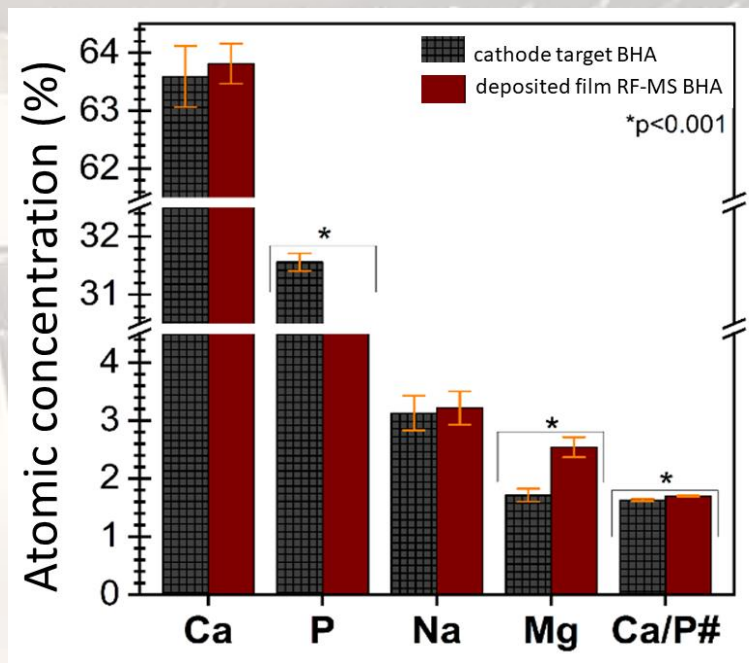
Ti6Al4V cranial mesh before (a) and after (b) the biofunctionalization with thin layers of HAB by RF-MS

Physico-chemical characterization of HAB films deposited by RF-MS



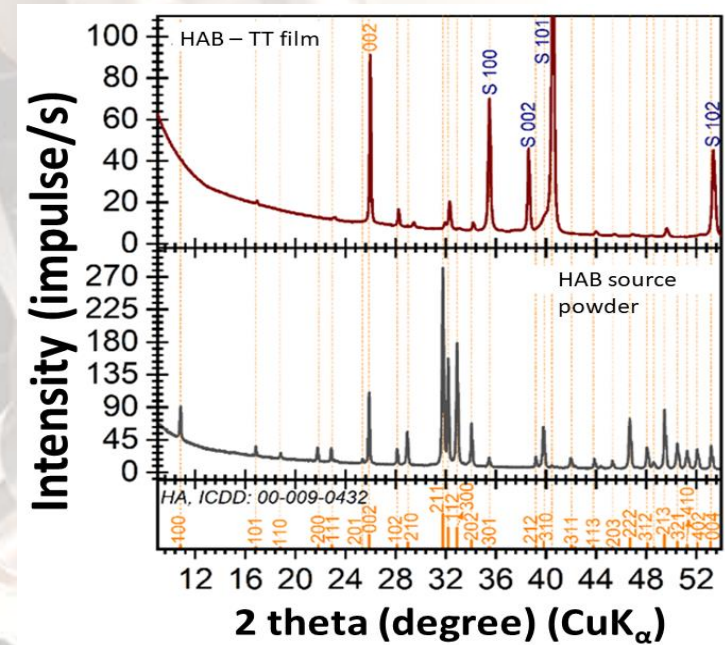
AFM images characteristic of the surface of HAB films acquired on areas of: (a) $25 \times 25 \mu\text{m}^2$; (b) $10 \times 10 \mu\text{m}^2$; (c) $5 \times 5 \mu\text{m}^2$; and (d) $2 \times 2 \mu\text{m}^2$

- polyhedral grains with diameters $\sim 110\text{-}230 \text{ nm}$
- RRMS of the HAB film surface is $\sim 15 \text{ nm}$



The elemental composition of the HAB film produced by RF-MS presented in comparison with the concentration of the target powder (estimated by EDXS measurements).

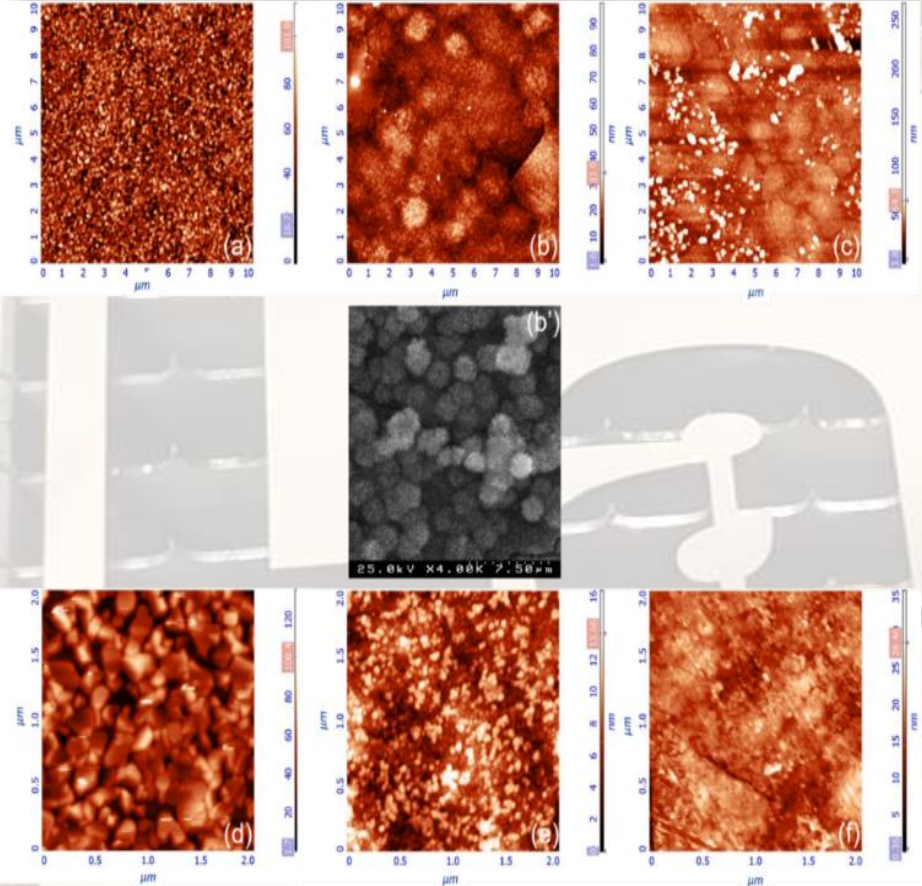
Ca/P source = 1.63 ± 0.02
 Ca/P HAB = 1.70 ± 0.01



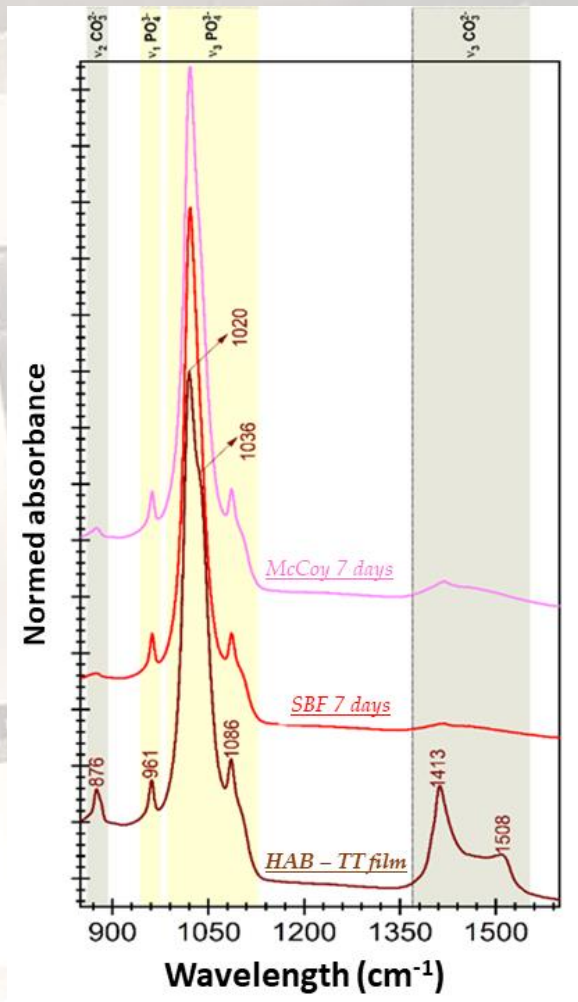
The comparative GIXRD diagrams of HAB single deposited (SD) film and heat-treated (TT) post-deposition at $500^\circ\text{C}/1\text{h}$ in air, acquired in incidence. At the bottom of the figure is the purely Synthetic Hydroxyapatite ICDD reference sheet (PDF4: 00-009-0432).

-were highlighted only well defined peaks of hydroxyapatite phase hexagonal crystal that shows a strong preferential orientation, the planes (002) parallel to the substrate

In vitro tests in simulated physiological solutions



AFM images characteristic of surface films HAB (A, D) before and after (b, c, e, f) immersing for 7 days in biological environments simulated type (b, e) SBF and (c, f) McCoy, procured aryl of: (a-c) $10 \times 10 \mu\text{m}^2$ and (d-f) $2 \times 2 \mu\text{m}^2$. (b') SEM image characteristic of the biomimetic hydroxyapatite layers formed in SBF [G.E. Stan et al; J. Mater. Sci.–Mater. Med, 2010]



Comparative FTIR spectra of the HAB heat-treated (TT) film at $500^\circ \text{C} / 1\text{h}$ in air before and after in vitro testing in SBF and McCoy simulated physiological solutions.

ISO 23317/2014: „Implants for surgery – In vitro evaluation for apatite-forming ability of implant material”

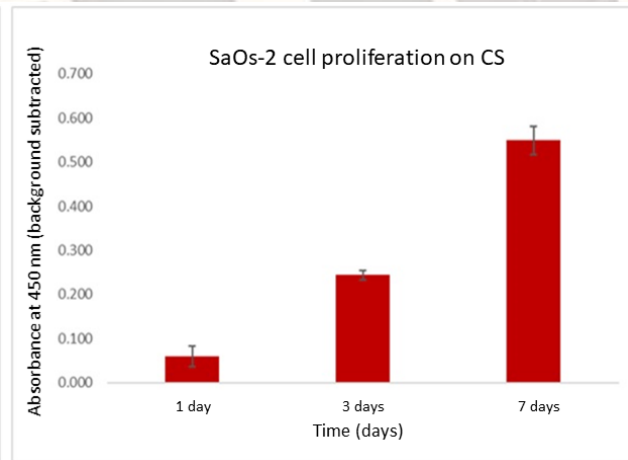
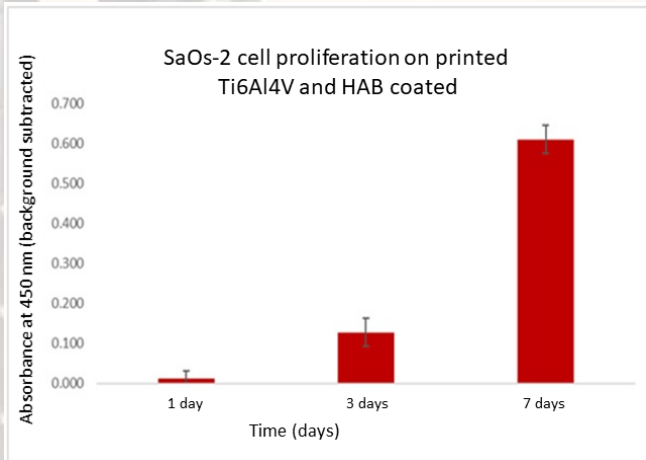


In vitro cytokine compatibility assays in osteoblast-like cell cultures

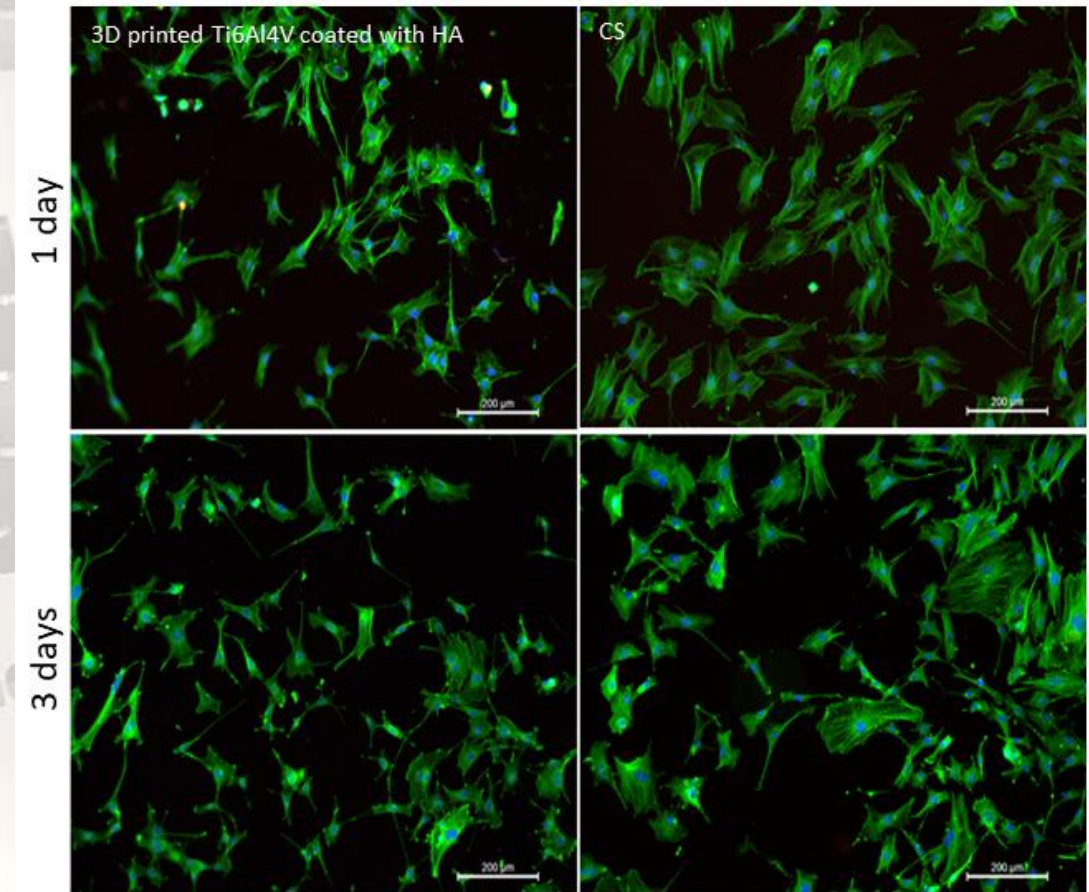


MTS assay

- tetrazolium salts degraded by viable cells → formazan → the production of formazan is proportional to the number of living cells
- Se verifica prin spectrofotometrie absorbanta la 450 nm. Cu cat absorbanta e mai mare inseamna c e mai mult formazan format → mai multe celule active.



Proliferation of SaOS-2 cells on 3D Ti6Al4V printed 3D coated HAB and CS, respectively, after 1 day, 3 days and 7 days after sowing.



Immunofluorescence images on 3D printed Ti6Al4V and covered with HAB (left column) and positive control (right column) 1 and 3 days after cultivation. The actin filaments - green, the nucleus - blue.



Conclusions



- Am generat prin imprimare 3D proteze metalice din Ti6Al4V. Am produs corpuri masive sub forma unor placute spinale prin tehnica de imprimare LMD si structuri discontinue sub forma unor mese craniene prin tehnica SLM
- Structura Ti6Al4V depusa prin SLM a fost martensitica α' , iar cea imprimata prin LMD a fost de tip α si β cu graunti martensitici α crescuti intr-o matrice de faza β
- Atat in cazul imprimarii SLM cat si a imprimarii LMD, am optimizat parametrii de iradiere astfel incat sa obtinem forme fara defecte, precum pori sau crapaturi si cu raspandire omogena a elementelor aliajului in volumul acestuia
- Protezele produse prin imprimare 3D au fost acoperite prin RF-MS cu un strat subtire de hidroxiapatita de origine animala
- Materialul s-a dovedit bioactiv, celulele de osteosarcom proliferand de la 1-7 zile si modificandu-si forma prin intindere si emitere de filopode

Laser Materials Processing Laboratory



Future research



- identificarea unor substraturi ceramice refractare compatibile cu Ti si aliajele sale, care sa reduca pasii tehnologici pentru obtinerea protezelor.
- studii *in vitro* amanuntite la nivel celular pentru determinarea precisa a comportamentului celulelor fata de straturile bioactive cu care vor intra in contact;
- studii *in vivo* pe animale pentru testarea functionarii in medii de viata reale.

Laser Materials Processing Laboratory

A black and white photograph showing a laser cutting machine in operation. The machine's nozzle is positioned over a metal plate. The plate has the word 'LAMIP' cut out in large, bold letters. Below the word, the text 'Laser Materials Processing Laboratory' is printed. At the bottom of the plate, the words 'Thank you!' are written in a stylized font. The machine's nozzle is currently cutting the letter 'P'. A ruler is visible at the bottom of the frame, showing measurements from 5 to 35.

LAMIP

Laser Materials Processing Laboratory

Thank you!